



PERGAMON

Available online at [www.sciencedirect.com](http://www.sciencedirect.com)

SCIENCE @ DIRECT®

Vision Research 43 (2003) 1765–1775

Vision  
Research

[www.elsevier.com/locate/visres](http://www.elsevier.com/locate/visres)

## Macular pigment density and distribution: comparison of fundus autofluorescence with minimum motion photometry

Anthony G. Robson <sup>a,f</sup>, Jack D. Moreland <sup>b</sup>, Daniel Pauleikhoff <sup>c</sup>, Tony Morrissey <sup>d</sup>,  
Graham E. Holder <sup>a</sup>, Fred W. Fitzke <sup>d</sup>, Alan C Bird <sup>a</sup>, Frederik J.G.M. van Kuijk <sup>a,e,\*</sup>

<sup>a</sup> Moorfields Eye Hospital, City Road, London EC1V 2PD, UK

<sup>b</sup> MacKay Institute of Communication and Neuroscience, Keele University, Staffordshire ST5 5BG, UK

<sup>c</sup> St. Franziskus Hospital, 48145 Muenster, Germany

<sup>d</sup> Institute of Ophthalmology, 11-43 Bath Street, London EC1V 9EL, UK

<sup>e</sup> Department of Ophthalmology and Visual Sciences, University of Texas Medical Branch, Galveston, TX 77555-1106, USA

<sup>f</sup> Department of Optometry and Neuroscience, UMIST, Manchester M60 1QD, UK

Received 2 December 2002; received in revised form 31 March 2003

### Abstract

Macular pigment (MP) distribution profiles were measured for 18 subjects using a Moreland anomaloscope modified for motion photometry. The total amount of MP within the central 7° was estimated from the distribution profile by numerical integration. Fundus autofluorescence images were obtained for eight of these subjects using a scanning laser ophthalmoscope. Peak optical density of MP increased with the total amount present, but the correlation was weakened by inter-subject differences in MP distribution. The mean MP distribution derived from mean grey-scale profiles of fundus autofluorescence images correlated closely with that obtained psychophysically ( $r = 0.96$ ). Autofluorescence imaging provides a fast non-invasive method for assessing MP in vivo.

© 2003 Elsevier Science Ltd. All rights reserved.

**Keywords:** Macular pigment; Imaging; Autofluorescence; Age-related macular degeneration; Motion photometry

### 1. Introduction

Macular pigment (MP) is a yellow carotenoid pigment found in both the inner and outer layers of the retina (Snodderly, Auran, & Delori, 1984; Snodderly, Brown, Delori, & Auran, 1984; Sommerburg et al., 1999) and is composed of two xanthophylls, lutein and zeaxanthin (Bone, Landrum, & Tarsis, 1985) that are derived from the diet (Sommerburg, Keunen, Bird, & van Kuijk, 1998). The role of MP is not fully understood. It may serve to reduce the effects of chromatic aberration and light scatter on visual performance (Nussbaum, Pruett, & Delori, 1981) although recent evidence suggests a minimal effect on retinal image quality (McLellan, Marcos, Prieto, & Burns, 2002). Importantly, it may have a protective role in screening photoreceptors from radiation damage by absorbing the

short wavelength high-energy photons (Snodderly, 1995) and by quenching reactive oxygen species, which are generated by light-activated photoreceptors (Beatty, Koh, Phil, Henson, & Boulton, 2000a, 2000b; Nussbaum et al., 1981). A protective role is consistent with findings that the pigmented area is less susceptible to short wavelength radiation damage than more eccentric areas (Ham, Ruffolo, Mueller, Clarke, & Moon, 1978; Lawwill, Crockett, & Currier, 1977; Weiter, Delori, & Dorey, 1988). There is also evidence that low levels of MP may be related to a higher risk of developing age-related macular degeneration (Beatty, Boulton, Henson, Koh, & Murray, 1999; Beatty et al., 2001; Bone et al., 2001; Landrum et al. 1997a, Landrum, Bone, & Kilburn, 1997b) and increasing attention has focused on the possibility of increasing MP levels through diet or dietary supplements (Berendschot et al., 2000; Bone, Landrum, Dixon, Chen, & Llerena, 2000; Ciulla et al., 2001a).

In many studies, in-vivo assessment of MP has relied on psychophysical techniques based on heterochromatic

\* Corresponding author. Tel.: +1-409-747-5411; fax: +1-409-747-5402.

E-mail address: [fjvankuij@utmb.edu](mailto:fjvankuij@utmb.edu) (F.J.G.M. van Kuijk).

flicker photometry (HFP) or motion photometry. Many have concentrated on the measurement of peak central absorbance (Beatty et al., 2000a, 2000b; Hammond, Fuld, & Snodderly, 1996; Landrum et al., 1997a, 1997b; Pease, Adams, & Nuccio, 1987) rather than MP spatial distribution, which may also vary between subjects (Hammond et al. 1997a, Hammond, Wooten, & Snodderly, 1997b; Moreland & Bhatt, 1984; Moreland, Robson, Soto-Leon, & Kulikowski, 1998; Vienot, 1983). MP measurements based on fundus imaging techniques allow assessment of larger retinal areas (Abadi & Cox, 1992; Kilbride, Alexander, Fishman, & Fishman, 1989) and offer additional advantages in terms of speed, patient comfort and convenience.

The main object of this study was to assess inter-subject differences in macular pigmentation in terms of peak density, extent of lateral distribution and total amount and to test the accuracy and validity of an imaging technique based on autofluorescence by reference to the established technique of motion photometry.

## 2. Methods

Macular pigment spatial distribution profiles were obtained in a series of healthy subjects using the psychophysical minimum motion paradigm (Moreland, 1982, 1983; Moreland, Robson, & Kulikowski, 2001; Moreland et al., 1998). Fundus autofluorescence images (Lois, Halfyard, Bird, & Fitzke, 2000; von Rückmann, 1995, 1999) were obtained for a subset of those subjects and MP profiles derived from those images were compared with those obtained psychophysically.

### 2.1. Psychophysical measurement of macular pigmentation using motion photometry

A modified Moreland anomaloscope (Moreland, 1980; Moreland & Kerr, 1979; Moreland & Young, 1974) was used in which a square wave grating (spatial frequency 0.38 c/deg) was moved at constant horizontal velocity (frequency  $\sim 14$  Hz, 37 deg/s). The grating was generated through the use of a spiral mirror mounted within the photometer head of the instrument (Moreland, 1980; Moreland & Todd, 1987). Alternate bars of the grating were illuminated using narrow-band interference filters (three-cavity, nominal half-height bandwidth 10 nm) with center wavelengths at 460 nm (maximum MP absorption) and 580 nm (zero MP absorption). Luminance matched filters (450 nm) were added to both elements to saturate S-cones. Stops were used to define a central circular field (diameter 0.8°) and 11 eccentric annular fields (range: 0.8°–7.4° eccentricity). The circular stimulus was fixated foveally and the annular stimuli were located parafoveally in the upper visual field while fixating centrally on a small dim red light.

Using the minimum motion paradigm, the radiance of the 580 nm stimulus was adjusted to minimize the perceived motion. Observations by 18 subjects with normal colour vision (screened with the Farnsworth-Munsell 100-Hue test) were made five times for each eye and for each field in single sessions of about 1 h. Relative absorbance for each eye was computed from  $\log(R_{\text{ref}}/R)$ , where  $R_{\text{ref}}$  is the mean radiance setting for the three most eccentric locations (5.5°, 6.6° and 7.4°) and  $R$  is the radiance setting at any location. Averaging across three eccentric locations reduces possible errors associated with the use of eccentric stimuli (see below) and provides a working reference for each eye session. The 580 nm radiance calibration was established using a LMT (Lichtmesstechnik Luminance meter L1000) photometer.

The total amount of MP (total MP within a three-dimensional MP profile) was estimated by integrating the two-dimensional spatial distribution profiles obtained for each subject and by assuming radial symmetry (this is supported by the preliminary imaging studies below). Apart from two subjects the profiles used were means for the left and right eyes and, where available, for multiple sessions (see Fig. 1). Since the angular sampling was coarse, interpolated values at 0.02° intervals were obtained from a mathematical function (a best-fit logistic, first or second order exponential or fourth order polynomial, as appropriate for each subject) to facilitate numerical integration. The value of this function at the most eccentric location was used to re-define zero MP absorbance (see below).

### 2.2. Fundus autofluorescence with a scanning laser ophthalmoscope

Autofluorescence (AF) images were obtained using a Zeiss prototype (SM 30-4024) confocal scanning laser ophthalmoscope (cSLO). This illuminated the fundus with argon laser radiation (488 nm, 250  $\mu$ W). The induced AF was viewed through a long-pass filter with a short-wavelength cut-off (50% transmission at 521 nm,  $1 \times 10^{-5}$  transmission at 495 nm, Coherent-Ealing Europe Ltd., Schott filter 0G515). The primary fluorophore at the excitation wavelength is believed to be lipofuscin at the level of the RPE (Delori et al., 1995; Eldred & Katz, 1988). The cSLO images were recorded at standard video scanning rates and digitized at  $256 \times 256$  resolution. Thirty-two individual images of each fundus were digitized at 6 frames/s and averaged to reduce noise. Anatomical landmarks such as retinal blood vessels were used as reference points for accurate alignment before averaging (von Rückmann, 1995, 1999).

The topographic distribution of AF across the retina was measured using a grey-scale index of intensity (0–255 units), along the vertical and horizontal meridians,

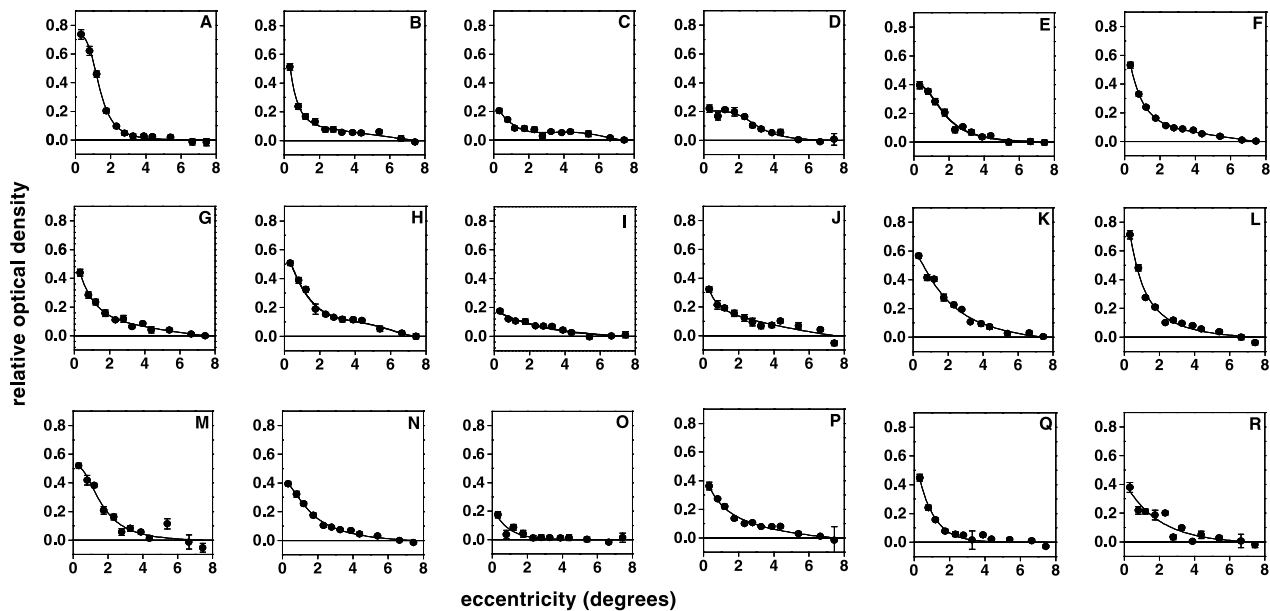


Fig. 1. MP spatial profiles obtained using motion photometry for a circular field (radius  $0.4^\circ$ ) and for eccentric annular segments presented in the superior visual field. Data obtained for the central circular field are plotted at  $0.3^\circ$  eccentricity to account for visual integration (see Section 4). Points are means for two eyes except for H and K and multiple sessions for A (5), B (3), C (2), E (4) and H (2). Curves are best-fit functions; logistic, first or second order exponential or fourth order polynomial. Zeros are set by the function value at  $7.4^\circ$ . Error bars represent  $2 \times$  mean sessional sem, computed from  $(\sum[\text{sem}]^2/n)^{0.5}$  where  $n$  is the number of eye-sessions (e.g.  $n = 3$  for subject H). In most cases doubled error bars are smaller than symbols. Subjects D, E, J, M, O and Q were female, the others were male.

intersecting the foveal pixel. The grey-scale intensity was calculated as the mean value for a  $20 \times 20$  ( $1^\circ$ ) pixel box. This area was chosen for comparison with the similar central area tested psychophysically and was centered on retinal locations between  $0^\circ$  and  $9.0^\circ$  eccentricity. Along the inferior vertical axis these retinal locations included areas assessed psychophysically.

Calibration of the grey scale was provided over more than 2 log units using a fluorescence standard (Avalon Technologies SFS-225) excited and recorded through the cut-off filter by the cSLO and simultaneously measured by a UDT (Universal Detector Technology) radiometer by reflecting a fraction from a glass cover slip. The relation between the grey scale and radiometer readings could accurately be described by a modified logistic function.

Relative optical density was calculated as  $\log(R_7/R)$ , where  $R_7$  is the radiance equivalent of the mean grey-scale value at  $7^\circ$  and  $R$  is the radiance equivalent value at any eccentricity.  $R_7$  was calculated from the mean of 1016 pixels, arranged in a 1 pixel-wide  $7^\circ$  circle centered on the fovea. This reduces the effect of artifacts due to retinal blood vessels, which encroached on the pigmented area of the macula in some subjects (see below). Optical density values may therefore be negative if the grey-scale value at any eccentricity is greater than the mean value at  $7^\circ$  eccentricity. Optical density values were multiplied by 1.28 in order to compensate for the difference between MP absorbance at 488 and 460 nm (Stockman, Sharpe, & Fach, 1999). Angular scaling of

AF profiles was determined for each subject by counting the number of individual pixels between the optic disc center and the fovea and converting to  $15^\circ$ .

### 3. Results

#### 3.1. Spatial profiles of macular pigment obtained using motion photometry

Fig. 1 shows MP profiles obtained using motion photometry from 18 subjects aged between 24 and 65 years. No subject had retinal eye disease and all subjects had normal color-discrimination (100-hue). In this figure, the provisional working zero (set using  $R_{\text{ref}}$ , the mean radiance setting for the three most eccentric locations) is reset more precisely by using the best-fit function value at  $7.4^\circ$ .

Pigment absorbance (optical density) in the central  $0.4^\circ$  varied between approximately 0.2 and 0.8 (subjects O and A); these values are plotted at  $0.3^\circ$  eccentricity to account for the effects of visual integration across the  $0.4^\circ$ —radius central field (see Section 4). Significant variation in distribution is also seen; relative absorbance dropped to zero at values between approximately  $2^\circ$  and  $7^\circ$  eccentricity. Distribution profiles varied from bell-shaped with domed peaks (subjects A, D and M) to trumpet shaped with sharp cusped peaks (subjects B, F, L and Q). Some profiles showed signs of a parafoveal shoulder (subjects C and H). In most individuals,

inter-ocular differences were small: point-by-point comparison of MP distribution between eyes reveals a high degree of inter-ocular symmetry ( $r^2 = 0.91$ ). This is consistent with biochemical measurements of MP (Handelman, Dratz, Reay, & van Kuijk, 1988). However, peak relative absorbance and the lateral extent of pigmentation were poorly correlated (Fig. 2).

Peak relative absorbance is more strongly related to total MP but a linear correlation accounts for only 23% of the variance (Fig. 3). This variability results from inter-subject differences in MP distribution, e.g. subjects H and Q, (Fig. 1) who have similar peak values of MP optical density (0.51 and 0.45) but dissimilar distribution

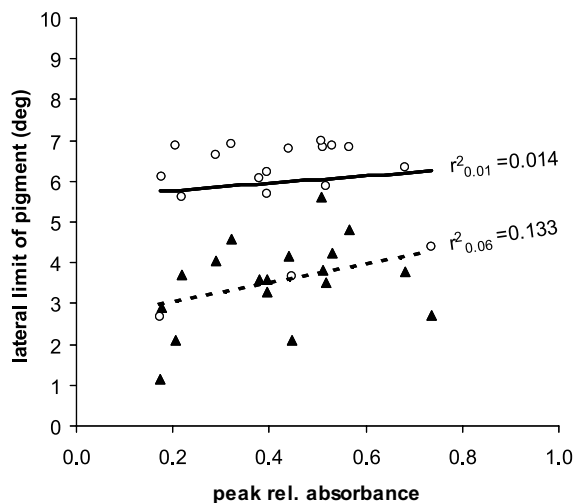


Fig. 2. Peak relative absorbance and the lateral limit of MP. Values are taken from Fig. 1 and the lateral extent of MP is measured according to the eccentricity at which relative absorbance of pigment is reduced to a relative optical density value of 0.01 (open circles,  $r = 0.12$ ) or 0.06 (filled triangles,  $r = 0.36$ ).

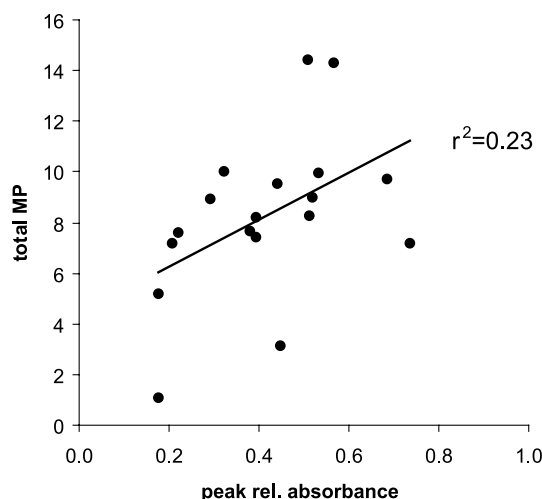


Fig. 3. Estimated total integrated MP as a function of peak relative absorbance. Peak absorbance is relative to  $7.4^\circ$ . A linear regression accounts for only 23% of the variance.

profiles resulting in a more than fourfold difference in total MP. Consequently, the total MP complement cannot be reliably predicted only from peak absorbance in individual subjects (Fig. 3), indeed such a prediction may lead to underestimation of total MP by ignoring lateral distribution (see below).

### 3.2. The effects of lateral distribution of macular pigment on peak absorbance measurements

MP profiles in Fig. 1 are calculated relative to the best-fit function value at  $7.4^\circ$  eccentricity. The aim in this part of the study was to simulate the effects of using less eccentric reference locations in order to examine potential errors in peak absorbance measurements caused by broad MP distributions. The variability evident in Fig. 3 is due to inter-subject differences in the shape of the MP profile and this is exacerbated by the use of less eccentric reference locations. The correlation between peak absorbance (relative to an eccentric reference) and total MP (within the central  $7.4^\circ$ ) decreases as the eccentricity of the reference location is reduced. For example, the coefficient of determination ( $r^2$ ) falls to 0.12 and 0.06 respectively for reference locations at  $4^\circ$  and  $2^\circ$  eccentricity.

Fig. 4 illustrates how reducing the eccentricity of the reference location to  $2^\circ$  or  $4^\circ$  leads to underestimation of peak optical density in some subjects (by up to 80% and 27% respectively). The reduction in computed peak absorbance is greatest for subjects with low levels of pigmentation, since laterally distributed MP constitutes a proportionately greater fraction of their MP complement.

MP may extend beyond  $7^\circ$ , as suggested by systematic trends in some profiles (most notably subjects B, C, F, G, H, K, L and P, Fig. 1). However, the psycho-

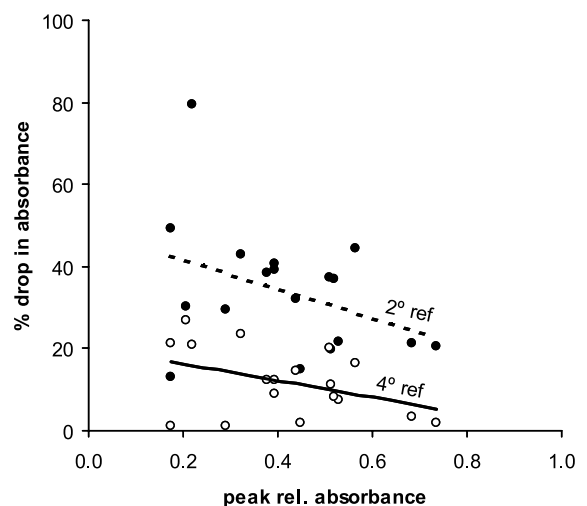


Fig. 4. Loss in apparent absorbance when using reference locations  $2^\circ$  (filled circles) or  $4^\circ$  (open circles) instead of  $7.4^\circ$ .

physical determination of MP beyond  $7^\circ$  eccentricity is complicated by the limiting characteristics of peripheral vision e.g. Troxler's fading and possible rod intrusion (Moreland & Bhatt, 1984). The assessment of MP beyond  $7^\circ$  requires a different technique (see below).

### 3.3. Assessment of macular pigment using fundus autofluorescence

Eight of the subjects tested using motion photometry were selected for fundus autofluorescence imaging (Fig. 1, subjects A–H). Fig. 5 shows autofluorescence images from one eye of these subjects. Since MP reduces the intensity of the 488 nm laser exciting radiation, fluorescence from regions of the retina with MP is reduced and these areas appear dark in the image. Areas of low MP density surround the fovea and inter-subject differences in the lateral extent of low MP density areas are evident (Fig. 5, first and third columns).

Relative optical density values of AF images were derived from a  $20 \times 20$  pixel box, at inferior retinal meridional locations corresponding with the upper visual field eccentricities used in the psychophysical de-

termination of MP distribution (Fig. 1) plus  $8^\circ$  and  $9^\circ$  eccentricity. Similar derivations were made along the superior meridian (approaching the edge of some AF images) and along the temporal and nasal meridians. Fig. 5 (second and fourth columns) shows the resulting spatial distribution profiles. Localized peaks in intensity, along the arms of the distribution curves, are present in most subjects, especially along the vertical meridians, that intersect the vascular arcades. In subject B there are prominent local peaks along both the superior and inferior profiles at  $5.4^\circ$  and  $4.4^\circ$  eccentricity respectively, which clearly correspond with retinal blood vessels visible in the AF image. Similar prominent peaks exist along the superior meridian of subject D (at  $5.4^\circ$  eccentricity) and along the superior and nasal profiles of subjects G and H. In subject C, one blood vessel is orientated vertically along the inferior meridian producing a plateau in the corresponding spatial profile at between  $5.4^\circ$  and  $7.4^\circ$ . If these artifacts are eliminated, there is a high degree of radial symmetry between the four meridians, as summarized in Fig. 6. If the foveal points (common to all meridians) are excluded, asymmetry is within  $\pm 8\%$  as estimated by the slopes of the

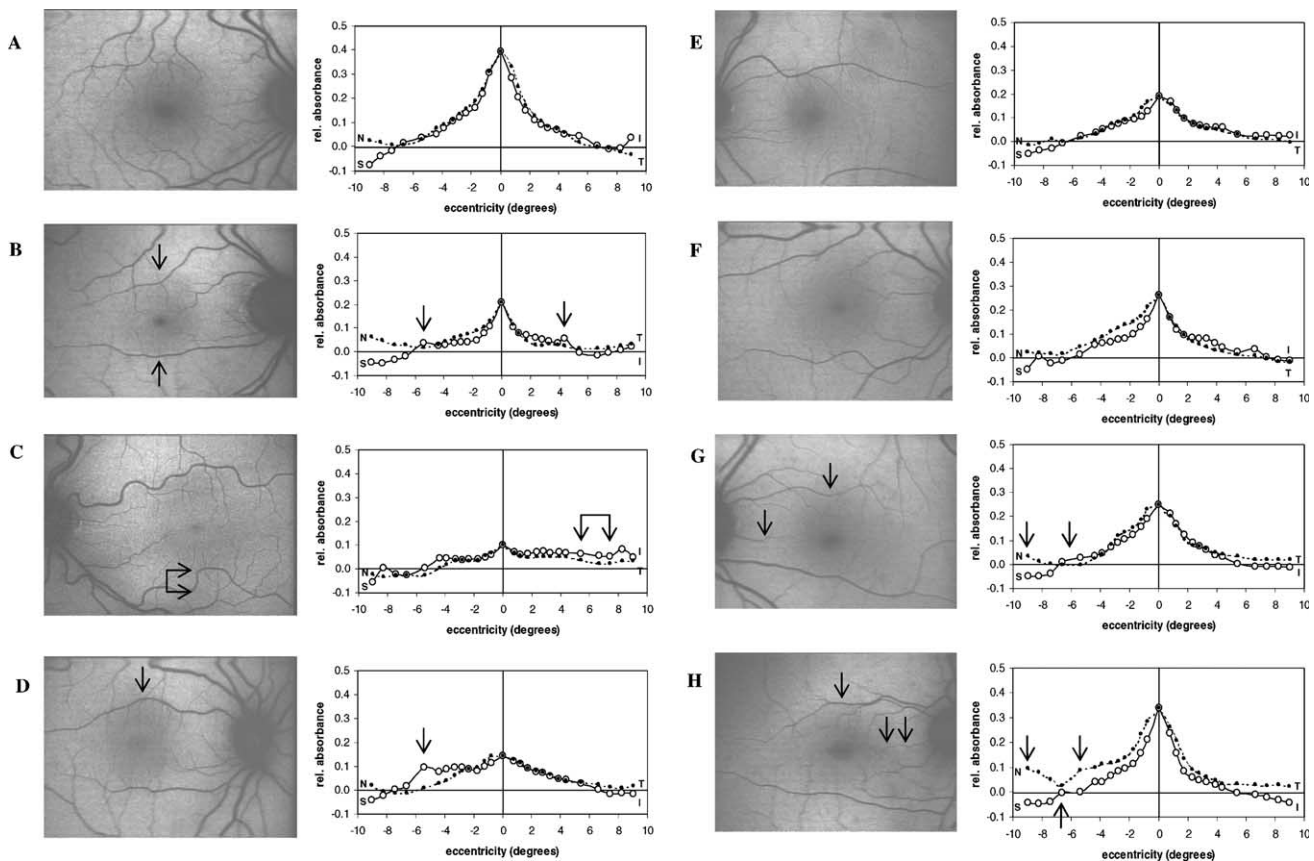


Fig. 5. Autofluorescence images (first and third columns) of subjects A–H and corresponding relative optical density profiles derived from mean grey-scale values (second and fourth columns). Open circles: superior (S)–inferior (I) meridian. Filled circles: nasal (N) and temporal (T) meridian. Superior and nasal eccentricities are negative. Arrows mark images and profiles where prominent blood vessels encroach on the  $20 \times 20$ -pixel areas. Optical density values are negative when the grey-scale value exceeds that of the reference (see Section 2).

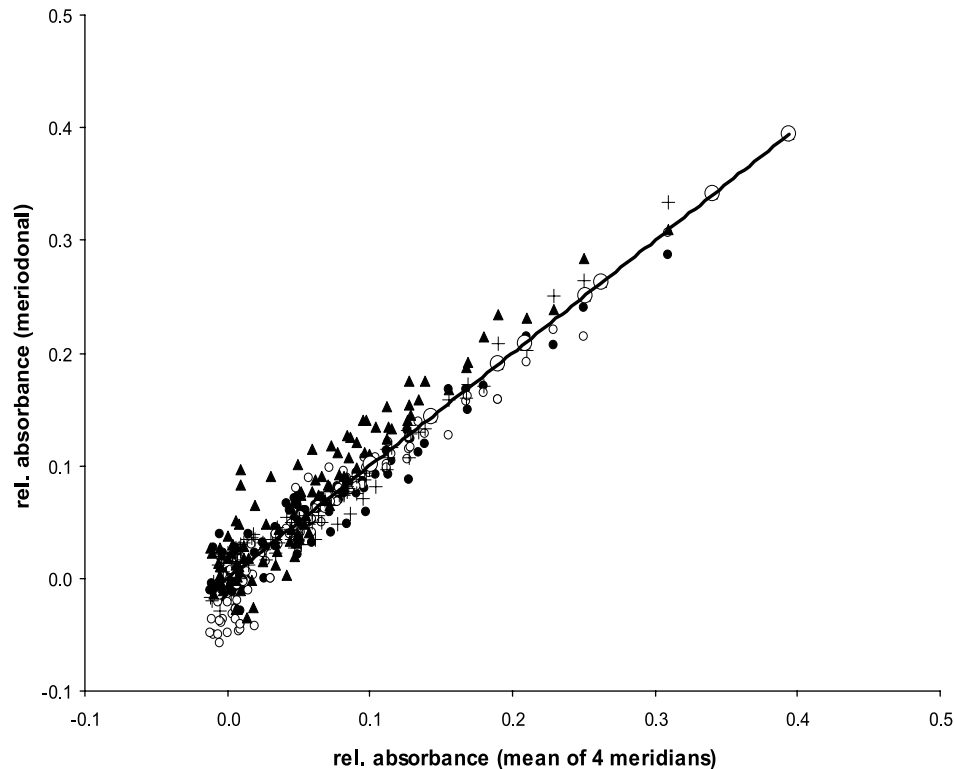


Fig. 6. Comparison of superior, inferior, nasal and temporal meridional absorbances with the meridional mean for AF images from eight subjects. Small open circles—superior, filled circles—inferior, crosses—temporal, triangles—nasal. Large open circles—fovea. Line—unit slope. Excluding foveal data, the slopes of the linear regressions are: 1.06 (superior), 0.92 (inferior), 1.08 (nasal) and 0.95 (temporal).

linear regressions of the individual meridians against the meridional mean. However, the slightly skewed profiles along the nasal–temporal meridian (subjects A, B and F) and along the superior–inferior meridian (subjects A, B, C, E, F and G) suggest the presence of an illumination gradient. Obtaining uniform illumination requires skill on the part of the cSLO operator, whose judgment is necessarily subjective. If this interpretation is correct and illumination gradients could be eliminated then retinal asymmetry would be considerably less than the aforementioned  $\pm 8\%$ .

The lateral extent of the low-density region lies within the central  $7.4^\circ$  in most subjects and along most meridians. In some cases, the presence of retinal blood vessels distort the spatial distribution profiles at the most eccentric retinal locations and impede the assessment of lateral extent. However, the low density area appears to extend beyond  $7.4^\circ$  in some cases: e.g., the superior meridians of subjects A, B, D, E, F, G and H; the temporal meridians of subjects A, E, and F and the inferior meridians of subjects F and H.

Superficially, there appears to be linear correlation between mean relative optical density derived from fundus autofluorescence and from motion photometry for the 12 retinal locations compared (Fig. 7). However, close examination reveals small eccentricity-dependent differences between the two sets of measurements. Lin-

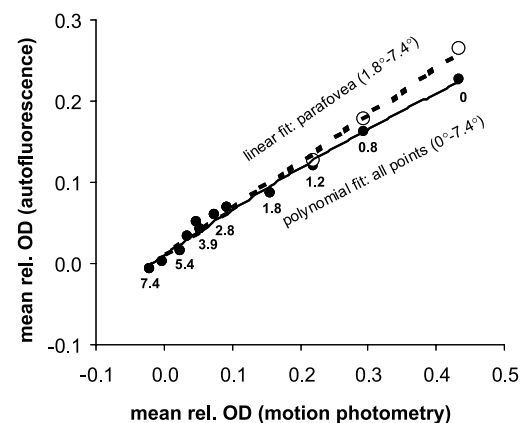


Fig. 7. Comparison of mean relative optical density of MP obtained by motion photometry and fundus autofluorescence at similar retinal locations. Filled circles—mean optical density values (eight subjects) at retinal locations between  $0^\circ$  and  $7.4^\circ$  eccentricity (labels are eccentricities in degrees). Filled circles are best fitted by a second order polynomial (solid line). Open circles—3 near-foveal points corrected by the difference between the linear and polynomial fits. Broken line—linear regression parafovea. The difference in shape between the central and extrafoveal regressions supports the observation that, for equal stimulation, there is less fluorescence foveally than elsewhere.

ear regression provides a best-fit for eccentricities greater or equal to  $1.8^\circ$ . All data (including values at  $1.2^\circ$ ,  $0.8^\circ$  and  $0^\circ$  eccentricity) are best fit by a second-

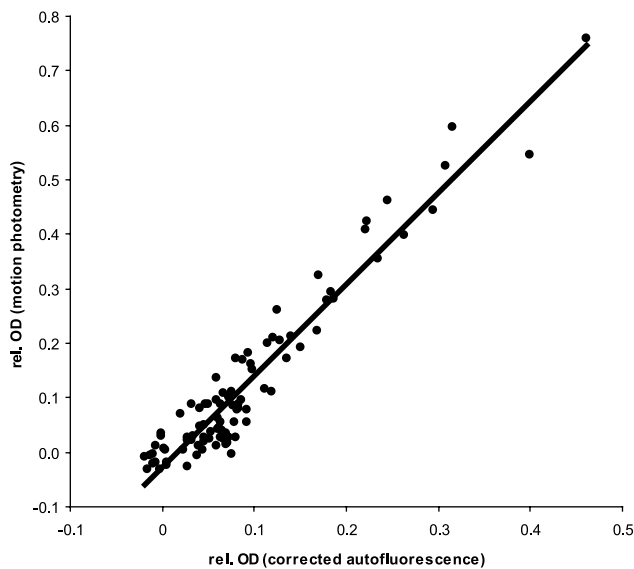


Fig. 8. Individual results (8 eyes  $\times$  12 retinal locations). Linear regression of motion photometry on autofluorescence. Slope = 1.7,  $r = 0.96$ .

order polynomial. The difference between linear and polynomial fits increases towards the fovea and can be interpreted in terms of a lower autofluorescence efficiency of the near foveal RPE. This small difference can be used as an eccentricity-dependent correction (Fig. 7,  $r = 0.99$ ). When applied to the eight subjects individually the correlation plot is linearised and provides a method of calibrating the AF technique (Fig. 8,  $r = 0.96$ ). This analysis indicates that the corrected AF optical density values should be multiplied by about 1.7 in order to predict psychophysically-derived absorbances.

#### 4. Discussion

Increasing interest in the relationship between MP and the pathogenesis of age related macular degeneration (e.g. Beatty et al., 1999) has led to numerous studies employing various psychophysical techniques to assess MP. Many of these methods use HFP and compare central sensitivity with that at a single more eccentric retinal location (Beatty et al., 2000a, 2000b; Ciulla et al., 2001a, 2001b; Hammond et al., 1996; Landrum et al., 1997a, 1997b; Pease et al., 1987; Wooten, Hammond, Land, & Snodderly, 1999). Although inter-subject variation in MP distribution has been recognized (Chen, Chang, & Wu, 2001; Hammond et al., 1997a, 1997b; Moreland & Bhatt, 1984; Moreland et al., 1998; Vienot, 1983) it is surprising that so many studies have ignored the possible effects of variable distribution in MP quantification.

The current study confirms the high degree of inter-subject variability both in terms of peak MP and dis-

tribution, and shows that the lateral extent, shape of distribution and total complement of MP cannot always be predicted from the peak absorbance values (Figs. 1–4). Estimates of the total complement of MP (as used in Fig. 3) are based on motion photometry measurements along a single meridian and computations assume that MP has a symmetrical distribution. A high degree of radial symmetry is confirmed by autofluorescence imaging (Figs. 5 and 6) validating such computations.

The current study utilises the technique of motion photometry, based on the phenomenon of motion nulling observed in the absence of luminance contrast (e.g. Cavanagh, Tyler, & Favreau, 1984; Lindsey & Teller, 1990; Ramachandran & Gregory, 1978; Stumpf, 1911). This technique yields measures of spectral sensitivity that are comparable with those obtained using HFP (Anstis & Cavanagh, 1983; Livingstone & Hubel, 1987; Moreland et al., 2001) and offers advantages in terms of ease of use and accuracy: direct comparison between minimum-flicker and minimum motion matches made by naïve subjects indicate that errors for motion matches are half those for flicker (Moreland, 1982; Moreland & Todd, 1987).

An important caveat in psychophysical studies is to choose a reference location that lies beyond the lateral extent of significant MP. Several recent psychophysical studies have used a reference location at  $4^\circ$  eccentricity (Ciulla et al., 2001a, 2001b; Hammond, Ciulla, & Snodderly, 2002; Wooten et al., 1999). It is clear from the current study that  $4^\circ$  or less will result in significant underestimation of peak MP in subjects with a broad MP distribution, particularly if pigmentation levels are low (Fig. 4). Since subjects with low levels of MP may be the most vulnerable to phototoxic light damage, the need for accurate MP quantification is crucial in such cases. It is evident that low levels of MP may extend beyond areas amenable to psychophysical measurement (Fig. 5). Fundus autofluorescence obviates this problem providing that intersubject differences in the reduction of AF across the macula is predominantly due to the effects of MP (Delori, Goger, Hammond, Snodderly, & Burns, 2001; see also Fig. 7) and the effects of the retinal vasculature are considered.

The motion photometry technique employed in this study minimizes contributions from S-cones and rods by using moderately high velocity motion ( $\sim 14$  Hz) and simultaneous 450 nm adaptation. Possible differences in L and M-cone distribution across the retina and the effects of photopigment optical density (Sharpe, Stockman, Knau, & Jagle, 1998; Vienot, 2001) are ignored. However, these effects are small. The effects of age-related lens yellowing (Pokorny, Smith, & Lutze, 1987; Ruddock, 1965, 1972; Said & Weale, 1959) on MP estimates have been modeled (Moreland et al., 2001). These effects are negligibly small since, with the use of narrow band stimuli, both central and para-central

measurements are affected nearly equally, even in extreme cases (Ciulla, Hammond, Yung, & Pratt, 2001b). Psychophysical techniques may underestimate peak values of MP if the photometric match for a central circular field is made at the edge of the stimulus (Hammond et al., 1997a, 1997b; Werner, Donnelly, & Kliegl, 1987) or if psychophysical performance is influenced by visual integration across the whole of the stimulus field. The latter may occur in color matching studies and results in matches equivalent to those made for an annulus at 70–80% of the central circular field radius (Moreland & Alexander, 1997). The current comparative study addresses this potential pitfall by calculating optical density in AF images from mean grey values over a  $20 \times 20$ -pixel area (a  $1^\circ$  square) that approximately corresponds with the retinal area assessed psychophysically. Peak values in Fig. 1, obtained using a circular field (radius  $0.4^\circ$ ), are therefore plotted at  $0.3^\circ$  eccentricity. Both the motion photometry fields and the AF sampling box attenuate localized foveal peaks in MP density, as revealed by preliminary assessments based on single pixel profiles across the macula (data not shown). The use of mean pixel values also reduces the possible confounding influence of MP granularity.

The present AF technique could over-estimate the total amount and/or the lateral extent of MP if the areas of low density represent additional absorbance by melanin at the level of the RPE or absorption by retinal hemoglobin. The difference in shape between the central and extrafoveal regressions (Fig. 7) also suggests that, for equal stimulation, there is less fluorescence foveally than elsewhere, in accord with preliminary in-vitro studies which compare AF before and after removal of the neurosensory retina (Losch, Jorzik, & Holz, 2001). The effects of these confounding variables have been assessed in studies utilizing longer wavelengths that are not absorbed by MP (Delori et al., 2001). Preliminary analysis of in-vivo images obtained using longer wavelength light confirms the prevalent effect of MP at shorter wavelengths (Delori, in preparation). Also, the AF measurements may be influenced by absorption at wavelengths longer than the cut-off of the SLO barrier filter. However, the close correlation between MP obtained from motion photometry and from AF suggests that the low density areas routinely observed in AF images are predominantly a consequence of MP, mildly accentuated in central areas by reduced autofluorescence efficiency (Fig. 7).

Even after correction for eccentricity dependent variation in autofluorescence (Figs. 7 and 8) autofluorescence assessment of MP requires the introduction of a coefficient to correct for underestimation of about 40% compared with psychophysical measurements (Fig. 8). The relationship described by Fig. 8 ( $r = 0.96$ , slope = 1.7) is comparable with the findings of Delori et al. (2001) that showed a lower correlation ( $r = 0.77$ ,

slope = 1.7) presumably resulting from methodological differences e.g., in the latter study, the imaging and minimum flicker techniques compute optical density relative to that at  $7^\circ$  and  $5.5^\circ$  eccentricity respectively, ignoring possible inter-subject differences in MP levels between these retinal locations (evident in the current study, Figs. 1 and 5).

The current study employs an SLO that images a  $40^\circ$  field. This allows accurate superimposition of individual images according to the retinal vasculature and ensures that the whole of the macula (and MP) is available for analysis. Other physical methods of assessing MP include fundus reflectance of the central  $1.5^\circ$  (Berendschot et al., 2000) or  $2^\circ$  (Wustemeyer, Jahn, Nestler, Barth, & Wolf, 2002), Raman spectroscopy of the central  $3^\circ$  (Bernstein, Yoshida, Katz, McClane, & Gellermann, 1998; Gellermann et al., 2002) and fundus autofluorescence within a  $2^\circ$  field (Delori et al., 2001). All of these methods may underestimate the total complement of MP (see Fig. 3) since the lateral distribution of MP has been assumed by the authors to be less significant or predictable from the peak value.

Spatial distribution is an important variable when estimating macular pigmentation since there are considerable differences in its lateral extent (Figs. 1, 2 and 5). Therefore, the total amount cannot always be inferred from the central peak concentration. This may have broad implications when patients vulnerable to ARMD are screened or when epidemiological studies on the role of MP in ARMD are conducted based on psychophysical methods employing measurement of peak MP. There is evidence that the parafoveal area is most vulnerable to phototoxic light damage (Ham et al., 1978; Lawwill et al., 1977; Weiter et al., 1988) and susceptibility may therefore be influenced by levels of MP at both the fovea and parafoveal locations. Current interest in dietary modification of MP (Berendschot et al., 2000; Bone et al., 2000, 2001; Ciulla et al., 2001a, 2001b; Curran-Celentano et al., 2001; Hammond et al., 1997a, 1997b) has often relied on monitoring peak MP levels, ignoring lateral distribution which may be an important factor, particularly in view of the different distribution profiles of zeaxanthin and lutein in man and macaque (Bone, Landrum, Fernandez, & Tarsis, 1988; Snodderly, Handelman, & Adler, 1991). Other studies, aimed at monitoring the effects of lutein supplementation on MP, while demonstrating the reliability of cSLO images compared with fundus reflectance and HFP, have also ignored the lateral distribution of MP (Berendschot et al., 2000).

Until the role of MP in the etiology of ARMD is understood it would seem prudent to assess pigmentation in terms of peak density, total MP and distribution for both epidemiological and screening purposes. The current data suggest that fundus autofluorescence provides an effective and accurate means of estimating the



distribution and therefore the total MP complement as well as the peak optical density, variables that cannot always be quantified psychophysically. In our experience the cSLO imaging methods are considerably faster and less demanding on the patient than psychophysical methods. These advantages may reduce variability in epidemiological studies and are likely to improve reliability in screening for susceptibility to ARMD.

## 5. Conclusions

This comparative study shows that MP distribution profiles vary between subjects. Accurate psychophysical assessment of MP requires the use of an eccentric reference location beyond that of significant lateral MP. Fundus autofluorescence provides a fast, non-invasive method of accurately assessing the density, distribution and total complement of MP in healthy subjects.

## Acknowledgements

A.G. Robson is supported by The Foundation Fighting Blindness. F.J.G.M. van Kuijk is supported by Research to prevent blindness. We are indebted to Professor J.J. Kulikowski and Chris Hogg for their help in preliminary studies.

## References

- Abadi, R. V., & Cox, M. J. (1992). The distribution of macular pigment in human albinos. *Investigative Ophthalmology and Visual Science*, 33, 494–497.
- Anstis, S., & Cavanagh, P. (1983). A minimum motion technique for judging equiluminance. In J. D. Mollon, & L. T. Sharpe (Eds.), *Colour vision* (pp. 155–166). London: Academic Press.
- Beatty, S., Boulton, M., Henson, D., Koh, H. H., & Murray, I. J. (1999). Macular pigment and age related macular degeneration. *British Journal of Ophthalmology*, 83, 867–877.
- Beatty, S., Koh, H., Phil, M., Henson, D., & Boulton, M. (2000a). The role of oxidative stress in the pathogenesis of age-related macular degeneration. *Survey of Ophthalmology*, 45, 115–134.
- Beatty, S., Koh, H. H., Carden, D., & Murray, I. J. (2000b). Macular pigment optical density measurement: a novel compact instrument. *Ophthalmic and Physiological Optics*, 20, 105–111.
- Beatty, S., Murray, I. J., Henson, D. B., Carden, D., Koh, H. H., & Boulton, M. E. (2001). Macular pigment and risk for age-related macular degeneration in subjects from a northern European population. *Investigative Ophthalmology and Visual Science*, 42, 439–446.
- Berendschot, T. T., Goldbohm, R. A., Kloppe, W. A., van de Kraats, J., van Norel, J., & van Norren, D. (2000). Influence of lutein supplementation on macular pigment, assessed with two objective techniques. *Investigative Ophthalmology and Visual Science*, 41, 3322–3326.
- Bernstein, P. S., Yoshida, M. D., Katz, N. B., McClane, R. W., & Gellermann, W. (1998). Raman detection of macular carotenoid pigments in intact human retina. *Investigative Ophthalmology and Visual Science*, 39, 2003–2011.
- Bone, R. A., Landrum, J. T., & Tarsis, S. L. (1985). Preliminary identification of the human macular pigment. *Vision Research*, 25, 1531–1535.
- Bone, R. A., Landrum, J. T., Fernandez, L., & Tarsis, S. L. (1988). Analysis of the macular pigment by HPLC: Retinal distribution and age study. *Investigative Ophthalmology and Visual Science*, 29, 843–849.
- Bone, R. A., Landrum, J. T., Dixon, Z., Chen, Y., & Llerena, C. M. (2000). Lutein and zeaxanthin in the eyes, serum and diet of human subjects. *Experimental Eye Research*, 71, 239–245.
- Bone, R. A., Landrum, J. T., Mayne, S. T., Gomez, C. M., Tibor, S. E., & Twaroska, E. E. (2001). Macular pigment in donor eyes with and without AMD: A case-control study. *Investigative Ophthalmology and Visual Science*, 42, 235–240.
- Cavanagh, P., Tyler, C. W., & Favreau, O. E. (1984). Perceived velocity of moving chromatic gratings. *Journal of the Optical Society of America A*, 1, 893–899.
- Chen, S., Chang, Y., & Wu, J. (2001). The spatial distribution of macular pigment in humans. *Current Eye Research*, 23, 422–434.
- Ciulla, T. A., Curran-Celantano, J., Cooper, D. A., Hammond, B. R., Jr., Danis, R. P., Pratt, L. M., Riccardi, K. A., & Filloon, T. G. (2001a). Macular pigment optical density in a midwestern sample. *Ophthalmology*, 108, 730–737.
- Ciulla, T. A., Hammond, B. R., Jr., Yung, C. W., & Pratt, L. M. (2001b). Macular pigment optical density before and after cataract extraction. *Investigative Ophthalmology and Visual Science*, 42, 1338–1341.
- Curran-Celantano, J., Hammond, B. R., Jr., Ciulla, T. A., Cooper, D. A., Pratt, L. M., & Danis, R. B. (2001). Relation between dietary intake, serum concentrations, and retinal concentrations of lutein and zeaxanthin in adults in a Midwest population. *American Journal of Clinical Nutrition*, 74, 796–802.
- Delori, F. C., Dorey, C. K., Staurenghi, G., Arend, O., Goger, D. G., & Weiter, J. J. (1995). In vivo fluorescence of the ocular fundus exhibits retinal pigment epithelium lipofuscin characteristics. *Investigative Ophthalmology and Visual Science*, 36, 718–729.
- Delori, F. C., Goger, D. G., Hammond, B. R., Snodderly, D. M., & Burns, S. A. (2001). Macular pigment density measured by autofluorescence spectrometry: comparison with reflectometry and heterochromatic flicker photometry. *Journal of the Optical Society of America A*, 18, 1212–1230.
- Eldred, G. E., & Katz, M. L. (1988). Fluorophores of the human retinal pigment epithelium: separation and spectral characterization. *Experimental Eye Research*, 47, 71–86.
- Gellermann, W., Ermakov, I. V., Ermakova, M. R., McClane, R. W., Zhao, D. Y., & Bernstein, P. S. (2002). In vivo resonant Raman measurement of macular carotenoid pigments in the young and the aging human retina. *Journal of the Optical Society of America A*, 19, 1172–1186.
- Ham, W. T., Ruffolo, J. J., Mueller, H. A., Clarke, A. M., & Moon, M. E. (1978). Histologic analysis of photochemical lesions produced in rhesus retina by short-wave-length light. *Investigative Ophthalmology and Vision Science*, 17, 1029–1035.
- Hammond, B. R., Ciulla, T. A., & Snodderly, D. M. (2002). Macular pigment density is reduced in obese subjects. *Investigative Ophthalmology and Vision Science*, 43, 47–50.
- Hammond, B. R., Fuld, K., & Snodderly, D. M. (1996). Iris color and macular pigment optical density. *Experimental Eye Research*, 62, 293–297.
- Hammond, B. R., Jr., Johnson, E. J., Russell, R. M., Krinsky, N. I., Yeum, K. J., Edwards, R. B., & Snodderly, D. M. (1997a). Dietary modification of human macular pigment density. *Investigative Ophthalmology and Vision Science*, 37, 1795–1801.
- Hammond, B. R., Wooten, B. R., & Snodderly, D. M. (1997b). Individual variations in the spatial profile of human macular pigment. *Journal of the Optical Society of America A*, 14, 1187–1196.

- Handelman, G. J., Dratz, E. A., Reay, C. C., & van Kuijk, F. J. G. M. (1988). Carotenoids in the human macula and whole retina. *Investigative Ophthalmology and Vision Science*, 29, 850–855.
- Kilbride, P. E., Alexander, K. R., Fishman, M., & Fishman, G. A. (1989). Human macular pigment assessed by imaging fundus reflectometry. *Vision Research*, 29, 663–674.
- Landrum, J. T., Bone, R. A., Joa, H., Kilburn, M. D., Moore, L. L., & Sprague, K. E. (1997a). A one year study of the macular pigment: The effect of 140 days of a lutein supplement. *Experimental Eye Research*, 65, 57–62.
- Landrum, J. T., Bone, R. A., & Kilburn, M. D. (1997b). The macular pigment: A possible role in protection from age related macular degeneration. *Advances in Pharmacology*, 38, 537–556.
- Lawwill, T., Crockett, S., & Currier, G. (1977). Retinal damage secondary to chronic light exposure, thresholds and mechanisms. *Documenta Ophthalmologica*, 44, 379–402.
- Lindsey, D. T., & Teller, D. Y. (1990). Motion at isoluminance: discrimination/detection ratios for moving isoluminant gratings. *Vision Research*, 30, 1751–1761.
- Livingstone, M. S., & Hubel, D. H. (1987). Psychophysical evidence for separate channels for the perception of form, colour, movement and depth. *Journal of Neuroscience*, 7, 3416–3468.
- Lois, N., Halfyard, A. S., Bird, A. C., & Fitzke, F. W. (2000). Quantitative evaluation of fundus autofluorescence imaged “in vivo” in eyes with retinal disease. *British Journal of Ophthalmology*, 84, 741–745.
- Losch, A. J., Jorzik, J., & Holz, F. G. (2001). Mapping of macular pigment distribution and RPE lipofuscin in human donor eyes with a confocal scanning laser ophthalmoscope (cSLO). *Investigative Ophthalmology and Visual Science*, 42(Suppl.), 221.
- McLellan, J. S., Marcos, S., Prieto, P. M., & Burns, S. A. (2002). Imperfect optics may be the eye's defence against chromatic blur. *Nature*, 417, 174–176.
- Moreland, J. D. (1980). A modified anomaloscope using optokinetic nystagmus to define colour matches objectively. In G. Verriest (Ed.), *Colour vision deficiencies V* (pp. 189–191). Hilger: Hilger.
- Moreland, J. D. (1982). Spectral sensitivity measurements by motion photometry. *Documenta Ophthalmologica Proceedings Series*, 33, 61–66.
- Moreland, J. D. (1983). Motion photometry. In J. Schanda (Ed.), *Proceedings of the 20th session of the international commission on illumination* (pp. 4–19). Amsterdam: Elsevier.
- Moreland, J. D., & Alexander, E. C. (1997). Effect of macular pigment on colour matching with field sizes in the 1°–10° range. *Documenta Ophthalmologica Proceedings Series*, 59, 363–368.
- Moreland, J. D., & Bhatt, P. (1984). Retinal distribution of macular pigment. *Documenta Ophthalmologica Proceedings Series*, 39, 127–132.
- Moreland, J. D., & Kerr, J. (1979). Optimization of a Rayleigh-type equation for the detection of tritanomaly. *Vision Research*, 19, 1369–1375.
- Moreland, J. D., Robson, A. G., & Kulikowski, J. J. (2001). Macular pigment assessment using a colour monitor. *Colour Research and Application*, 26(Suppl.), 261–263.
- Moreland, J. D., Robson, A. G., Soto-Leon, N., & Kulikowski, J. J. (1998). Macular pigment and the colour-specificity of visual evoked potentials. *Vision Research*, 38, 3241–3245.
- Moreland, J. D., & Todd, D. T. (1987). Motion photometry and the spectral sensitivity of colour defectives. In E. Marré, M. Tost, & H. J. Zenker (Eds.), *Normal and pathologic vision* (pp. 39–42). Halle: Martin-Luther Universität.
- Moreland, J. D., & Young, W. B. (1974). A new anomaloscope employing interference filters. *Modern Problems in Ophthalmology*, 13, 47–55.
- Nussbaum, J. J., Pruett, R. C., & Delori, F. C. (1981). Historic perspectives Macular yellow pigment. The first 200 years. *Retina*, 1, 296–310.
- Pease, P. L., Adams, A. J., & Nuccio, E. (1987). Optical density of human macular pigment. *Vision Research*, 27, 705–710.
- Pokorny, J., Smith, V. C., & Lutze, M. (1987). Aging of the human lens. *Applied Optics*, 26, 1437–1440.
- Ramachandran, V. S., & Gregory, R. (1978). Does colour provide an input to human motion perception? *Nature*, 275, 55–56.
- Ruddock, K. H. (1965). The effect of age upon colour vision. II. Changes with age in light transmission of the ocular media. *Vision Research*, 5, 47–58.
- Ruddock, K. H. (1972). Light transmission through the ocular media and macular pigment and its significance for psychophysical investigation. In L. M. Hurvich, & D. Jameson (Eds.), *Handbook of sensory physiology VII* (pp. 455–469). Heidelberg: Springer Verlag.
- Said, F. S., & Weale, R. A. (1959). The variation with age of the spectral transmissivity of the living human crystalline lens. *Gerontologia*, 3, 213–231.
- Sharpe, L. T., Stockman, A., Knau, H., & Jagle, H. (1998). Macular pigment densities derived from central and peripheral spectral sensitivity differences. *Vision Research*, 38, 3233–3239.
- Snodderly, D. M. (1995). Evidence for protection against age-related macular degeneration by carotenoids and antioxidant vitamins. *American Journal of Clinical Nutrition*, 62(Suppl.), 1448–1461.
- Snodderly, D. M., Auran, J. D., & Delori, F. C. (1984). The macular pigment. II. Spatial distribution in primate retinas. *Investigative Ophthalmology and Visual Science*, 25, 674–685.
- Snodderly, D. M., Brown, P. K., Delori, F. C., & Auran, J. D. (1984). The macular pigment. I. Absorbance spectra, localization, and discrimination from other yellow pigments in primate retinas. *Investigative Ophthalmology and Visual Science*, 25, 660–673.
- Snodderly, D. M., Handelman, G. J., & Adler, A. J. (1991). Distribution of individual macular pigment carotenoids in central retina of macaque and squirrel monkeys. *Investigative Ophthalmology and Visual Science*, 32, 268–279.
- Sommerburg, O., Keunen, J. E. E., Bird, A. C., & van Kuijk, F. J. G. M. (1998). Fruits and vegetables that are sources for lutein and zeaxanthin: the macular pigment in human eyes. *British Journal of Ophthalmology*, 82, 907–910.
- Sommerburg, O., Siems, W. G., Hurst, J. S., Lewis, J. W., Klier, D. S., & van Kuijk, F. J. G. M. (1999). Lutein and zeaxanthin are associated with photoreceptors in the human retina. *Current Eye Research*, 19, 491–495.
- Stockman, A., Sharpe, L. T., & Fach, C. (1999). The spectral sensitivity of the human short-wavelength sensitive cones derived from thresholds and color matches. *Vision Research*, 39, 2901–2927.
- Stumpf, P. (1911). On the dependence of the visual sensation of movement and its negative aftereffect on the stimulation processes in the retina. Translated by D. Todorovic 1996. A gem from the past: Pleikart Stumpf's (1911) anticipation of the aperture problem, Reichardt detectors, and perceived motion loss at equiluminance. *Perception*, 25, 1235–1242.
- Vienot, F. (1983). Can variation in macular pigment account for the variation of colour matches with retinal position. In J. D. Mollon, & L. T. Sharpe (Eds.), *Colour vision. Physiology and psychophysics* (pp. 107–116). London: Academic Press.
- Vienot, F. (2001). Retinal distribution of the macular pigment and the cone effective optical density from colour matches of normal observers. *Colour Research and Application*, 26(Suppl.), 264–268.
- von Rückmann, A., Fitzke, F. W., & Bird, A. C. (1995). Distribution of fundus autofluorescence with a scanning laser ophthalmoscope. *British Journal of Ophthalmology*, 79, 407–412.
- von Rückmann, A., Fitzke, F. W., & Bird, A. C. (1999). Distribution of pigment epithelium autofluorescence in retinal disease state recorded in vivo and its change over time. *Graefes's archives of clinical and experimental ophthalmology*, 237, 1–9.

- Weiter, J. J., Delori, F., & Dorey, C. K. (1988). Central sparing in annular macular degeneration. *American Journal of Ophthalmology*, 106, 286–292.
- Werner, J. S., Donnelly, S. K., & Kliegl, R. (1987). Aging and human macular pigment density. *Vision Research*, 27, 257–268.
- Wooten, B. R., Hammond, B. R., Land, R. I., & Snodderly, D. M. (1999). A practical method for measuring macular pigment optical density. *Investigative Ophthalmology and Visual Science*, 40, 2481–2489.
- Wustemeyer, H., Jahn, C., Nestler, A., Barth, T., & Wolf, S. (2002). A new instrument for the quantification of macular pigment density: first results in patients with AMD and healthy subjects. *Graefes' archives of clinical and experimental ophthalmology*, 240, 666–671.